

# Lipid-polycaprolactone Core-shell Hybrid Nanoparticles for Controlled Delivery of Nateglinide

Punamjyoti Das, Malay K. Das

Department of Pharmaceutical Sciences, Dibrugarh University, Dibrugarh, Assam, India

## Abstract

**Objective:** Lipid-polymer hybrid nanoparticles (LPHNPs) combine the biomimetic advantages of lipids and the structural benefits of polymers. The aim of the present study is the development of core shell LPHNPs encapsulating a model lipophilic drug nateglinide and perceived its controlled delivery. **Materials and Methods:** LPHNPs were prepared by single emulsion solvent evaporation method using polycaprolactone as polymer and glyceryl monostearate, palmitic acid, and lauric acid as lipid. The formulations were characterized in terms of particle size, zeta potential, drug entrapment efficiency, drug loading (DL), surface morphology, *in vitro* drug release, and release kinetics studies. **Results:** Dynamic light scattering analysis demonstrated the smaller particle size of LPHNPs ( $380.2 \pm 3.5$ – $544.7 \pm 2.8$  nm) as compared to polycaprolactone polymeric NPs (PNPs) ( $647.1 \pm 1.9$ – $675.8 \pm 3.7$  nm). Transmission electron microscopy images of LPNPs and PNPs demonstrate that they are spherical in shape. The entrapment efficiencies ( $84.9 \pm 0.1$ – $87.76 \pm 0.23\%$ ) and DL capacity ( $4.63 \pm 0.01$ – $8.18 \pm 0.09\%$ ) of LPHNPs were higher than PNPs ( $72.5 \pm 0.1\%$  and  $2.05 \pm 0.005\%$ ). The higher colloidal stability of LPHNPs was confirmed by their zeta potential value at  $-12.5 \pm 2.1$ – $33.4 \pm 0.2$  mv as compared to zeta potential of PNPs ( $-8.71 \pm 0.3$ – $9.60 \pm 0.1$  mv). The LPHNPs displayed a biphasic drug release pattern with an initial burst release, followed by controlled release. The LPHNPs demonstrated the slower drug release (60–70% at 24 h) than that from PNPs (90% at 24 h). **Conclusion:** The results suggest the controlled release behavior of nateglinide from the developed lipid-polymer core shell hybrid NPs. The developed nanocarriers hold the great promise for controlled delivery of both the lipophilic and hydrophilic drugs to improve their pharmacokinetics.

**Key words:** Lipid-polymer hybrid nanoparticles, Polymeric nanoparticles, Nateglinide, Controlled release, Polycaprolactone

## INTRODUCTION

Nanotechnology represents a powerful tool in the medicinal zone, which has the potential to greatly impact the delivery of plenty of therapeutic and diagnostic imaging agents. It also holds a great promise for improving the pharmacokinetics and therapeutic index of a myriad of drugs.<sup>[1,2]</sup> Nanoparticles (NPs) have grabbed a great deal of attention as they are customizable for targeted delivery of drugs at desired times and doses.<sup>[3]</sup> Polymer and lipids are most often used materials for the purpose of developing these nanocarriers since both of these have their own advantages. Polymer-based systems include polymeric NPs, polymeric micelles, and polymer-drug conjugates and lipid-based systems include liposomes, nanostructured lipid carriers, and solid lipid nanoparticles.<sup>[4,5]</sup>

On comparing these two different matrices, it was observed that lipid-based carriers show advantages in terms of better compatibility, favorable pharmacokinetic profile, easy surface modification, however, suffers from limitations in terms of their stability, tedious sterilization process, a burst release of the drug and high polydispersity.<sup>[5,6]</sup> Polymeric carriers also provide several advantages such as small particle size, narrow size distribution, controlled drug release, reproducible manufacturing process, easy modification of the surface with different moieties, and improved stability. However, polymeric systems have certain limitations such as toxicity due to

### Address for correspondence:

Malay K. Das, Department of Pharmaceutical Sciences, Dibrugarh University, Dibrugarh Assam India.  
E-mail: mkdps@dibru.ac.in

Received: 02-10-2020

Revised: 11-03-2021

Accepted: 01-04-2021

polymer degradation products, use of organic solvents in the manufacturing process, and limited drug loading (DL).<sup>[7,8]</sup>

To counter the limitation associated with the other nanocarriers, a new colloidal carrier, which merges the advantages of both the polymeric and lipoidal nanocarriers, has been developed omitting few limitations of both the nanocarriers. This novel colloidal nanocarrier is known as "Lipid-Polymer Hybrid Nanoparticle."<sup>[9]</sup>

Lipid-polymer hybrid NPs (LPHNPs) is a rising nanoparticle drug delivery system. A superior drug delivery system has been yielded by combining the architectural benefits of polymer core and biomimetic properties of lipids.<sup>[10]</sup> LPHNPs are solid, submicron particles composed of two major components: Polymer cores and single or multiple lipid layers that compose the outer shells. LPHNPs comprise the characteristic of both the liposome and polymeric NPs.<sup>[11]</sup> In the LPHNPs, the polymer core is capable of encapsulating both hydrophilic and hydrophobic drugs and the inclusion of lipid coat enveloping the polymer core serves as a potential obstacle to restrict the fast leakage of drugs, hence prolonging and controlling the release of drugs.<sup>[12]</sup> LPHNPs exhibit multiple advantages including (1) diversity in the structural component, (2) improved stability profile, (3) superior capability of coencapsulating therapeutic and imaging agents of different properties, and (4) conjugation with targeting moieties. Due to these advantages, LPHNPs system is of tremendous potential for deliveries of a wide range of therapeutic agents.<sup>[13,14]</sup> Therefore, the present study takes the advantages of this nanocarrier to achieve controlled delivery of a model antidiabetic drug.

Nateglinide, 3-phenyl-2-[(4propan-2ylcyclohexane carbonyl) amino] propanoic acid [Figure 1] having molecular formula  $C_{19}H_{27}NO_3$ , is an oral hypoglycemic agent. It brings down the blood glucose level by stimulating insulin release from the pancreas as a result of the blockade of the ATP-dependent potassium channels present in the  $\beta$  cells membrane. It has a short half-life of 1.5 h, and is metabolized by the cytochrome P450 system. The 60 mg and 120 mg nateglinide immediate-release tablets are available in the market which necessitates the administration frequency of twice or thrice a day. To discard these pharmacokinetic limitations associated with nateglinide it was chosen as a model drug for controlled delivery.<sup>[15]</sup>

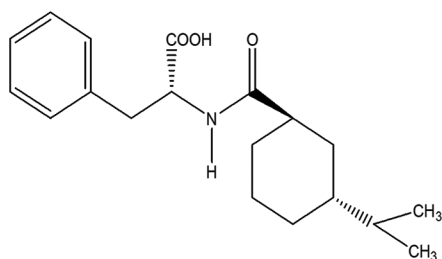


**Figure 1:** Chemical structure of nateglinide

The selection of the polymer for the core of LPHNPs is critical. Polycaprolactone (PCL) is one of the most widely employed FDA approved biodegradable and biocompatible polymer, which is non-toxic and has a great permeability to several drugs.<sup>[16]</sup> In this study, PCL forms the polymeric core for the encapsulation of drug molecules in hybrid NPs.

Lipid-based drug delivery system has drawn more interest due to its improved stability, the possibility of controlling drug release and drug targeting. In this present study, three lipids glyceryl monostearate (GMS), palmitic acid (PA), and lauric acid (LA) are used for surrounding the polymer core. All the lipids are saturated fatty acid with different carbon atom chain length that has high biocompatibility and non-toxicity. Lipids being part of the physiological composition deems them suitable for pharmaceutical use and can be adopted for engineering nanoparticle-based drug delivery carriers.<sup>[17,18]</sup>

In the present study, three novel LPHNPs with PCL as polymer core and GMS, PA, and LA, individually as monolayer lipid shells were prepared and evaluated. The optimized formulations were characterized for the physicochemical properties such as surface morphology, particle size, zeta potential, entrapment efficacy, and DL and *in vitro* drug release study. Polycaprolactone polymeric NPs (PNPs) were prepared to compare the parameters of developed LPHNPs. There are no literature reports on these combinations of polymer, lipids for nateglinide delivery. The objective of the present work is the investigation of these novel LPHNPs for their better entrapment efficiency/DL and improved morphological/architectural structure for promising controlled delivery of nateglinide.

## MATERIALS AND METHODS

### Materials

Nateglinide was received as a gift sample from Alembic Pharmaceutical Ltd., Vadodara, India. PCL was purchased from Sigma-Aldrich, India. GMS was purchased from Yarrow Chem Products, Mumbai, India. Polyvinyl Alcohol was purchased from LobaChemie Pvt. Ltd., Mumbai, India. Methanol, chloroform, PA, and mannitol were purchased from HiMedia Laboratories Pvt. Ltd., Mumbai, India. LA, Dichloromethane, and Sodium Hydroxide were purchased from Sisco Research Laboratories Pvt. Ltd., Mumbai, India. All the other reagents and chemicals used were of analytical grade.

### Methods

#### Preparation of LPHNPs

The LPHNPs were prepared by modified single emulsion solvent evaporation (ESE) method.<sup>[19-22]</sup> Briefly, drug, polymer, and lipid at different proportions [Table 1] were

**Table 1:** Formulation of nateglinide loaded LPHNPs

Formulation code	Lipid: polymer	Lipid: polymer Ratio	Dichloromethane (ml)	Amount of drug (mg)	Aqueous phase (ml)	Polyvinyl alcohol (%w/v)
LPHNPs (F1)	GMS: PCL	1:1	2	10	10	1
LPHNPs (F2)	PA: PCL	1:2	2	10	10	1
LPHNPs (F3)	LA: PCL	1:5	2	10	10	1

\*PCL: Polycaprolactone, GMS: Glycerylmonostearate, PA: Palmitic acid, LA: Lauric acid

dissolved in 2 ml of dichloromethane (DCM) in a beaker forming the oil phase. Then, 10 ml of PVA (1% w/v) solution was used as an aqueous phase which also performed as a stabilizing agent for the formulations. Afterward, the oil phase was added drop-wise in to the aqueous phase (1% w/v PVA, 10 ml) under constant stirring. The mixture was sonicated at 40 kHz frequency for 20 min with gentle heating at 20°C using a bath sonicator (Spectra lab Instrument Pvt. Ltd., Mumbai, India). The produced emulsion was placed on magnetic stirrer to evaporate DCM with constant stirring up to 4 h. The NPs were collected by centrifugation at 14,000 rpm for 15 min to collect the NPs. NPs were washed 3 times with distilled water and then resuspended in a fixed volume of water with cryoprotectant mannitol (5% w/v) and lyophilized (Lyophilizer SSI-140) at -80°C for 30 h to obtain the NPs. The blank LPHNPs and nateglinide loaded polymeric NPs (NTG-PNPs) were prepared by the same method.<sup>[23,24]</sup>

### Characterization of LPHNPs and PNPs

#### Particle size, polydispersity index (PDI), and zeta potential

The particle size and PDI of the LPHNPs, and PNPs were determined by dynamic light scattering using a Particle size analyzer (Brookhaven Instrument 90 Plus, USA). The surface charge of the LPHNPs and PNPs was estimated by the analysis of the zeta potential using a Zetasizer Nano ZS (Malvern Instruments, UK). Zeta potential is useful for physical stability assessment of the particle. For the size and zeta potential measurement, the dispersion of LPHNPs and PNPs was diluted with ultrapure water according to the mass concentration (1:100 w/v). All measurement was taken at 25°C and each sample was analyzed in triplicate.<sup>[25,26]</sup>

#### Drug entrapment and loading efficiency

To find out the drug entrapment and loading efficiency, 10 mg of lyophilized NPs were dissolved in 10 ml of phosphate buffer pH 6.8 for 24 h. After 24 h, the solution was filtered through using a 0.45 µm filter and the concentration of the nateglinide in the filtrate was determined spectrophotometrically at 207 nm using a UV-VIS spectrophotometer (Shimadzu UV-1800, Japan) against phosphate buffer pH 6.8 as a blank. The absorbance value was plotted on the previously prepared standard

curve ( $y = 0.037x + 0.015$ ,  $R^2 = 0.990$ ) to get the exact concentration of the drug and subsequently the practical drug content was calculated.<sup>[27,28]</sup>

$$\text{Drug Entrapment Efficiency (\%)} = \frac{\text{Practical Drug Content}}{\text{Theoretical Drug Content}} \times 100 \quad (1)$$

$$\text{Drug Loading (\%)} = \frac{\text{Practical Drug Content}}{\text{Total Weight of NPs Obtained}} \times 100 \quad (2)$$

### Drug-exciipient compatibility study

To determine any type of interaction between the drug and excipients, FT-IR, DSC, and XRD analysis of the individual component nateglinide, PCL, GMS, PA, and LA and NTG-loaded LPHNPs and polymeric nanoparticle were done.

The FT-IR analysis were done by placing the sample over the sample holder of the FT-IR spectrometer (Bruker Alpha, Germany) and scanning was done in the wavelength region between 4000 and 400  $\text{cm}^{-1}$ , to determine the presence and type of functional groups and chemical bonds.<sup>[29,30]</sup>

The DSC patterns of pure drug nateglinide, physical mixtures and nateglinide-loaded LPHNPs that are NTG-PCL-GMS (F1), NTG-PCL-PA (F2), and NTG-PCL-LA (F3) and PNPs were obtained and interpreted using Differential Scanning Calorimeter (DSC 4000, Perkin Elmer, USA). Around 5 mg of the sample was placed in a standard aluminum pan and heated across a temperature range of 40–250°C with a constant heating rate of 10°C per min. The DSC analysis generally used to examine the purity, thermal transitions, and compatibility of drug, lipid, and polymer.<sup>[31,32]</sup>

The effect of crystallinity of drug and excipients was studied using XRD analysis. The XRD patterns of NTG, physical mixture of NTG and excipients, lyophilized blank, and drug loaded LPHNPs and PNPs, were recorded using X-ray Diffractometer (Rigaku-Ultima IV, Japan), using copper radiation, voltage of 40 kV, and current of 30 mA. The scanning speed employed was 2°/min over the range of 0–60° diffraction angle.<sup>[31,33]</sup>

## Morphological characterization

Transmission electron microscopy (TEM) is the technique used to look at the internal and the external structure of the materials. To understand the internal structures of LPHNPs and PNPs, a drop of nanoparticle suspensions was placed onto a copper grid and air dried, followed by negative staining with 3% aqueous solution of sodium phosphotungstate as contrast agent. The air-dried samples were then directly examined under the TEM (HRTEM JEOL, JEM- 2100 Plus, Japan) at different resolutions.<sup>[34-36]</sup>

## In vitro drug release study

The *in vitro* release studies were performed using dialysis method for quantification of drug released from the LPHNPs and PNPs formulation. A sample of 1 ml NPs suspension, with a NTG concentration of 1 mg/ml, was sealed in a dialysis bag (HiMedia, Mumbai, India) having a pore size 2.4 nm, molecular weight cutoff 12,000–14,000 and dipped in 50 ml of phosphate buffer pH 6.8. During the experiment, the buffered solution was maintained at  $37 \pm 0.5^\circ\text{C}$  with a stirring speed of 100 rpm. After a definite interval of time, 5 ml of samples were withdrawn and analyzed for drug content using UV spectrophotometer (Shimadzu UV-1800, Japan) at 207 nm. The release studies were performed in triplicate for each formulation.<sup>[21,37,38]</sup>

## In vitro drug release kinetics

To examine the release mechanism of nateglinide from both the LPHNPs and PNPs, the *in vitro* drug release data were fitted into various kinetic models such as Zero order, First order, Higuchi, and Korsmeyer–Peppas (K-P) model. By comparing the observed  $R^2$  values, the best-fit model was picked up. Different mathematical equations for these models are as follows:<sup>[39]</sup>

$$\text{Zero order: } Q_t = Q_0 - K_0t \quad (3)$$

$Q_t$  = amount of drug released at time  $t$ ,  $Q_0$  = initial amount of drug in the formulation,  $K_0$  = zero order release constant at (concentration/time).

First order:

$$\log C = \log C_0 - \frac{K_1 t}{2.303} \quad (4)$$

$C_0$  = initial amount of drug in formulation,  $C$  = amount of drug remaining in the formulation at time  $t$ .

$$\text{Higuchi: } Q_t = K_H t^{1/2}$$

$Q_t$  = amount of drug release at time  $t$  per unit area,  $K_H$  = Higuchi release constant

$$\text{Korsmeyer - Peppas: } \frac{M_t}{M_\infty} = Kt^n \quad (5)$$

$\frac{M_t}{M_\infty}$  = fraction of drug release at the  $t$ ,  $K$  = release rate constant,  $n$  = release exponent

## Statistical analysis

The experimental results were expressed as mean  $\pm$  SD. Statistical significance was tested using Student's  $t$ -test and  $P < 0.05$  was considered to be statistically significant.

## RESULTS AND DISCUSSION

The NPs were prepared using different ratios of drug:lipid:polymer with varying amount of drug between 5 and 15 mg. The drug entrapment and DL efficiency were found to be low at smaller loading dose, whereas larger size of NPs was observed at higher loading dose. A higher drug entrapment and DL efficiency with desirable particle size was observed when the nateglinide loading dose was fixed at 10 mg along with the optimized lipid:polymer ratio [Table 1].

FT-IR analysis was used to identify any chemical interaction that occurred among the drug, polymer and lipids. The FT-IR Spectra of pure nateglinide, PCL, GMS, PA, LA, and their physical mixtures and also drug-loaded LPHNPs and PNPs formulations are shown in Figure 2. Nateglinide, PCL, glyceryl monostearate, PA, and LA show the characteristic band due to different functional groups, shown in Table 2.<sup>[40]</sup> By comparing the spectrum of the physical mixture with individual spectra of the drug, polymer, and lipid, it can be clearly seen that in the physical mixture nearly all the peaks of the individual compounds and drug existed, thus no interaction is detected in the physical mixture. However, in case of the spectrum of the optimized formulation LPHNPs (F1), the stretching vibration of C-O-C was decreasing from  $1162.55 \text{ cm}^{-1}$  to  $1154.23 \text{ cm}^{-1}$  and also in the LPHNPs (F2) spectra the stretching vibration of C=C was decreasing from  $1462.19 \text{ cm}^{-1}$  to  $1455.01 \text{ cm}^{-1}$ . Furthermore, in the LPHNPs (F3) spectra, the peak of a free hydroxyl group (for OH stretching) is not observed, which may be due to the interaction between the drug, polymer, and lipid molecules and the interaction is most probably an intermolecular hydrogen bonding between drug, polymer, and lipid leading to higher DL.

The DSC was carried out to detect the sample purity and also to determine whether the drug was incorporated in the LPHNPs and PNPs as crystalline or amorphous form. In Figure 3, the DSC thermogram demonstrated that pure nateglinide have a sharp endothermic peak at  $139.52^\circ\text{C}$  correspond to its melting point. PCL showed an endothermic peak at  $69.03^\circ\text{C}$ . The thermogram of GMS

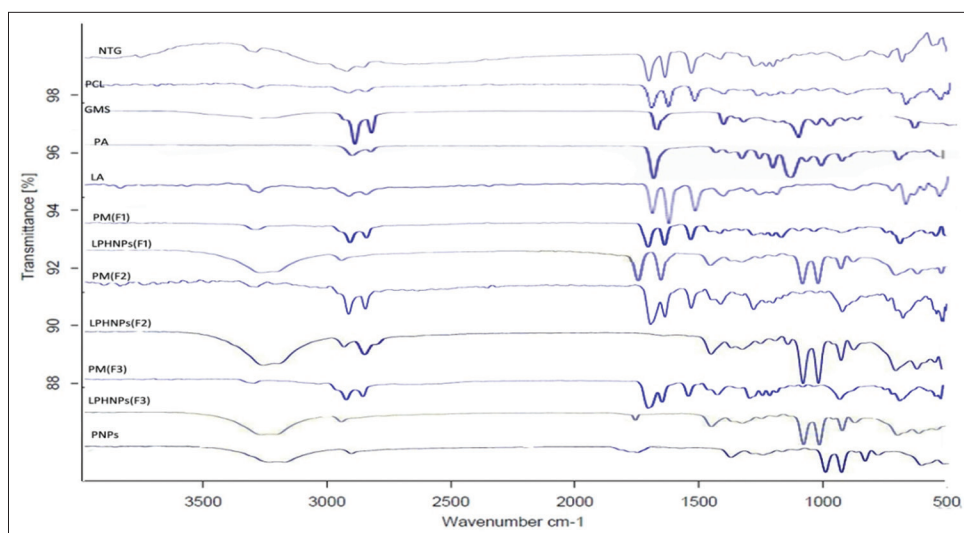


**Figure 2:** FT-IR spectrums of (A) Nateglinide (NTG), (B) Polycaprolactone (PCL), (C) Glyceryl monostearate (GMS), (D) Palmitic acid (PA), (E) Lauric acid (LA), (F) Physical mixture (PM(F1)), (G) LPHNPs(F1), (H) Physical mixture (PM(F2)), (I) LPHNPs(F2), (J) Physical mixture (PM(F3)), (K) LPHNPs(F3), (L) PNP<sub>s</sub>

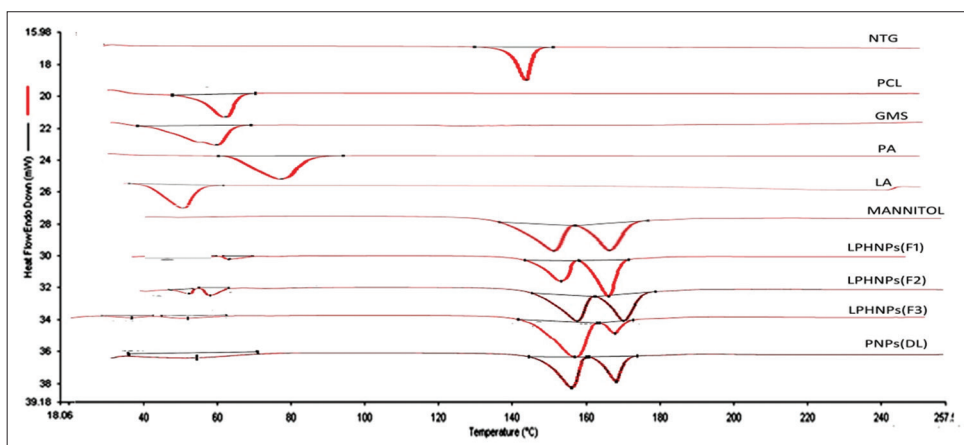


**Figure 3:** DSC thermograms of (A) Nateglinide (NTG), (B) Polycaprolactone (PCL), (C) Glyceryl monostearate (GMS), (D) Palmitic acid (PA), (E) Lauric acid (LA), (F) Mannitol, (G) LPHNPs(F1), (H) LPHNPs(F2), (I) LPHNPs(F3), (J) PNP<sub>s</sub>(DL)

and PA showed a broad endothermic peak at 66.23°C and 74.24°C, respectively. LA showed a sharp endothermic peak at 53.94°C. The thermogram of mannitol also showed two endothermic peaks at 157.48°C and 168.65°C. NTG-LPHNPs formulations showed endothermic peak corresponding to PCL, lipids and lyophilizing agent mannitol with no peak for NTG. And also NTG-PNP<sub>s</sub> showed the endothermic peak corresponding to PCL, and mannitol with no drug peak. This suggested that the encapsulated drug might exist in the polymer matrix as either amorphous form or disordered in crystalline form.<sup>[41-43]</sup>

The X-ray diffractogram of the pure drug nateglinide, PCL, GMS, PA, and LA showed a group of sharp peaks at 2–20°, 20–23°, 20–28°, 20–26°, and 20–25° (2θ), respectively, which is reflective of its crystalline nature. XRD of the optimized formulations F1, F2, F3, and PNP<sub>s</sub> are shown in Figure 4 and it is observed that in the drug-loaded LPHNPs and PNP<sub>s</sub> formulation the nateglinide peak is absent, which

indicate that the drug becomes amorphous or solubilize in the formulation matrix.<sup>[40,44]</sup>

The particle size, PDI and zeta potential of optimized LPHNPs (F1, F2, and F3) and polymeric NP<sub>s</sub> were determined and it was observed that particle size of LPHNPs was smaller than PNP<sub>s</sub>. The particle size of LPHNPs ranged from 380.2 ± 3.5 to 544.7 ± 2.8 nm and PNP<sub>s</sub> ranged from 615.9 ± 0.6 to 675.8 ± 0.96 nm. The size of NTG-LPHNPs and NTG-PNP<sub>s</sub> was larger than their blank formulations, which indicated the loading of the drug and results in enlarging the size of the nanocarriers. The size of the drug loaded and blank formulations was considered as statistically significantly different [ $P < 0.05$ , when done using two-tailed unpaired Student's *t*-test, Table 3].<sup>[34]</sup>

Zeta potential is indicative of the physical stability of formulations. Table 3 summarizes the particle size, PDI, and zeta potential of LPHNPs and PNP<sub>s</sub>. The zeta potential of the

**Table 2: FT-IR interpretation data of nateglinide and other excipients**

Standard wave number range (cm <sup>-1</sup> )	Type of the band	Observed wave number (cm <sup>-1</sup> )
<b>Nateglinide</b>		
3300–3600	N-H stretch	3286.26
≥ 3000	C-H stretch (sp <sup>2</sup> )	3021.67
≤ 3000	C-H stretch (sp <sup>3</sup> )	2926.58
1700	C=O stretch	1646.53
≥ 1700	COOH	1711.87
1250–1600	C=C	1540.73
1150–1250	C-O stretch	1244.69
1050–1250	C-N stretch	1214.06
<b>Polycaprolactone</b>		
2949	CH <sub>2</sub> stretching (asymmetric)	2940.72
2865	CH <sub>2</sub> stretching (symmetric)	2865.61
1727	C=O stretching	1720.93
1293	C-O and C-C stretching	1292.83
1162–1240	C-O-C ( symmetric and asymmetric)	1165.22,1238.40
1020–1250	C-N stretching	1142.08,1102.82
<b>Glycerol monostearate</b>		
1743	C=O stretching	1730.87
1000-1200	C-H stretching	1051.09,1104.39,1173.69
700–850	C-H bending	718.06
930–937	O-H stretching	942.96
<b>Palmitic acid</b>		
2853–2924	C-H stretching (symmetric and asymmetric)	2911.78
1650–1780	C=O stretching	1692.31
3300-2500	O-H stretching	3291.52
800–1300	C-C bond	933.22, 1283.96
<b>Lauric acid</b>		
2853–2924	C-H stretching (symmetric and asymmetric)	2853.60
1650–1780	C=O stretching	1710.80
1292	C-O stretching	1287.32
2500–3600	O-H stretching	2919.36
<b>Mannitol</b>		
2850–3000	C-H stretching	2912.20
1450–1470	C-H bending	1414.71
2500–3600	O-H stretching	3390.15
1050–1125	C-O stretching	1075.70

different formulations was consistently negative and in the range of –12–33 mv for LPHNPs and –8–9 mv for PNP. In general, a large positive or negative zeta potential (greater than +30 mV or less than –30 mV) is favorable for obtaining particles with better stability. Therefore, LPHNPs exhibit more stability than PNP. The advantage of using negatively charged LPHNPs is that particles are expected to be less toxic and more stable than positively charged NPs in the human body.<sup>[45,46]</sup> The zeta potential curves of the optimized formulations are depicted in Figure 5.

The drug encapsulation efficiency (EE) of the NPs is crucial for their clinical application. The nateglinide encapsulation capacity of LPHNPs ranged from 84.9 ± 0.1% to 87.76 ± 0.23% and DL of LPHNPs were ranged from 4.63 ± 0.01% to 8.18 ± 0.09%. Higher EE and DL were obtained in LPHNPs compared with polymeric NPs (*P* < 0.05). This higher EE and DL can be explained that lipid shell presented at the surface of the nateglinide-loaded PCL core can prevent small drug molecules from freely diffusing out of the polymeric core, thereby improving drug encapsulation and loading yield.<sup>[47]</sup>

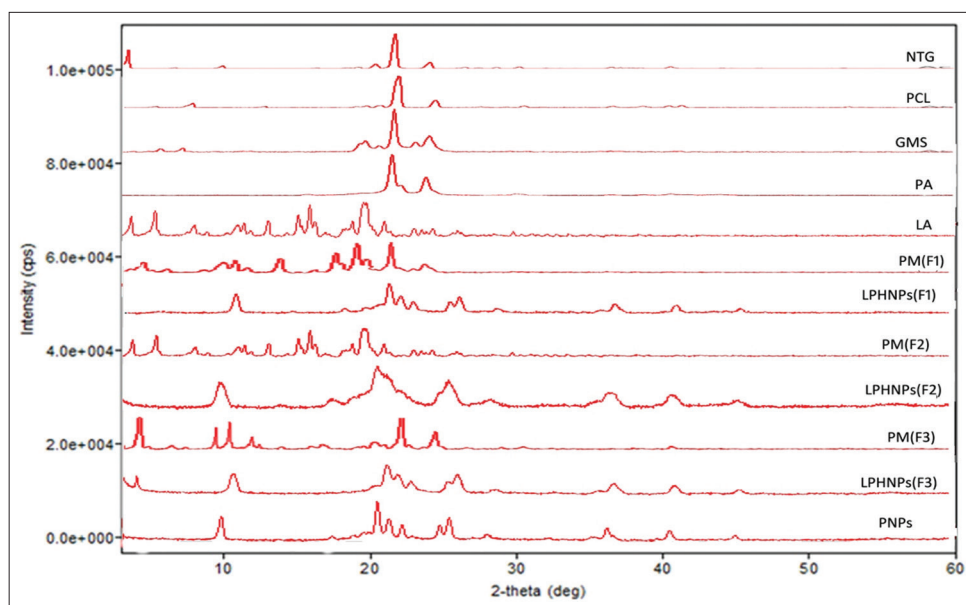


**Figure 4:** XRD thermograms of (A) Nateglinide (NTG), (B) Polycaprolactone (PCL), (C) Glyceryl monostearate (GMS), (D) Palmitic acid (PA), (E) Lauric acid (LA), (F) Physical mixture-1 (PM(F1)), (G) Drug loaded nanoparticles-1 (LPHNPs(F1)), (H) Physical mixture-2 (PM(F2)), (I) Drug loaded nanoparticles-2 (LPHNPs(F2)), (J) Physical mixture-3 (PM(F3)), (K) Drug loaded nanoparticles-3 (LPHNPs(F3)), (L) PNPs

**Table 3:** Particle size, polydispersity index, zeta potential, drug loading, and drug entrapment efficiency of the LPHNPs and PNPs

Formulation code	Particle size (nm)**	Polydispersity index	Zeta potential (mV)	Drug loading (%)	Entrapment efficiency (%)
LPHNP-F <sub>1</sub> (B)	430.3±4.1	0.271±0.08	-19.6±0.8	-	-
LPHNP-F <sub>1</sub> (DL)	451.4±2.4 <sup>a1</sup>	0.309±0.14	-33.4±0.2	8.18±0.09	87.76±0.23
LPHNP-F <sub>2</sub> (B)	487.5±4.2	0.300±0.07	-16.5±1.9	-	-
LPHNP-F <sub>2</sub> (DL)	544.7±2.8 <sup>a2</sup>	0.281±0.08	-28.4±0.7	7.26±0.02	87.13±0.25
LPHNP-F <sub>3</sub> (B)	316.9±5.1	0.434±0.12	-12.5±2.1	-	-
LPHNP-F <sub>3</sub> (DL)	380.2±3.5 <sup>a3</sup>	0.303±0.09	-18.4±0.5	4.63±0.01	84.9±0.1
PNPs (B)	647.1±1.9	0.385±0.10	-8.71±0.3	-	-
PNPs (DL)	675.8±3.7 <sup>a4</sup>	0.33±0.06	-9.60±0.1	2.05±0.005	72.5±0.1

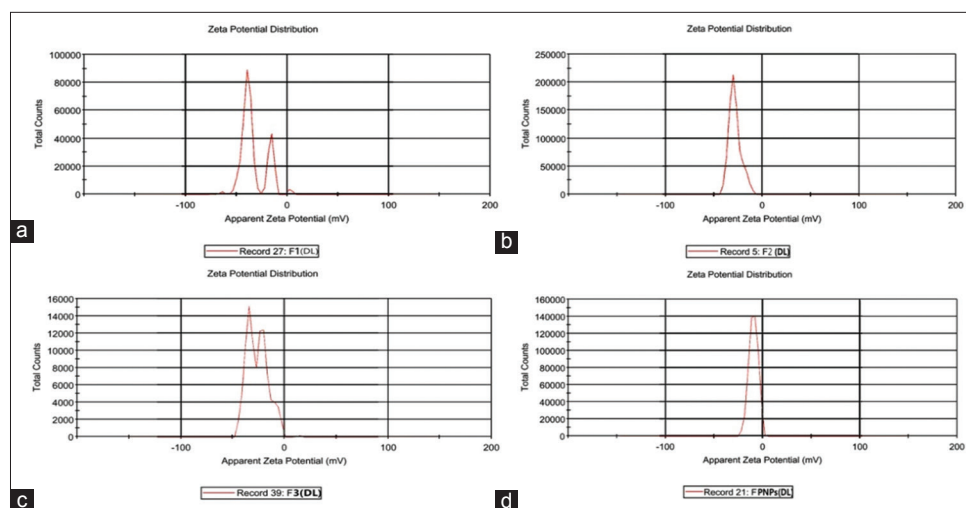
<sup>#</sup>B: Blank, DL: Drug loaded. Data are presented as mean±SD ( $n=3$ ). \*\*Data were significantly different ( $P<0.05$ ), when the size of the drug loaded nanoparticle and blank nanoparticle were compared by two tailed unpaired Student's  $t$ -test. <sup>a1</sup>Data were significantly different ( $P=0.004$ ), where drug loaded LPHNPs-F1 were compared with its blank formulation by two-tailed unpaired student's  $t$ -test. <sup>a2</sup>Data were significantly different ( $P=0.01$ ), where drug loaded LPHNPs-F2 were compared with its blank formulation by two-tailed unpaired student's  $t$ -test. <sup>a3</sup>Data were significantly different ( $P=0.03$ ), where drug loaded LPHNPs-F3 were compared with its blank formulation by two-tailed unpaired Student's  $t$ -test. <sup>a4</sup>Data were significantly different ( $P=0.02$ ), where drug loaded PNPs were compared with its blank formulation by two-tailed unpaired Student's  $t$ -test

Table 3 depicts the physicochemical properties of all the LPHNPs and PNPs formulations.

The internal as well as the external structure of the drug-loaded LPHNPs and PNPs was assessed by TEM, showed in Figure 6a-c. From TEM, it was observed that drug loaded LPHNPs clearly showed spherical shape, exhibiting a black spot surrounded by a transparent wall of a lipid monolayer. In the TEM study, the electron is transmitted through the sample but in case of polymer the electron not permeate through the polymer, hence it gives a black color spot, but in case of lipid the electron easily permeates and gives a transparent

or fated like structure.<sup>[20,48]</sup> In Figure 6d, PNPs have also exhibited as dark spot spherical shaped structure. Inside the spherical core of PNPs there was the presence of some dark dotted spot, which indicates the drug encapsulation in the polymeric core.

Drug release studies were performed using the dialysis membrane method in phosphate buffer pH 6.8 and maintain the temperature at  $37 \pm 0.5^\circ\text{C}$  with a stirring speed of 100 rpm. *In vitro* release profiles of LPHNPs were compared with PNPs and its drug release curves are displayed in Figure 7. The percentage drug release of LPHNPs formulations (F1, F2, and



**Figure 5:** Zeta potentials curve of drug loaded formulations (a) lipid-polymer hybrid nanoparticles (LPHNPs) F1, (b) LPHNPs F2, (c) LPHNPs F3, and (d) PNPs

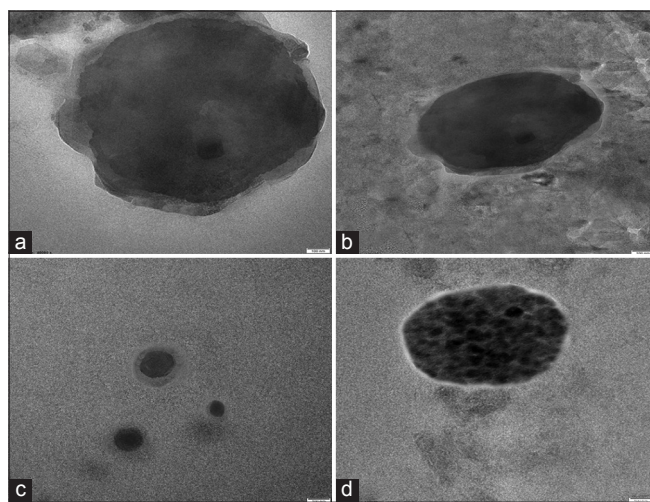


**Figure 6:** Transmission electron microscopy images of drug loaded formulations of (a) lipid-polymer hybrid nanoparticles (LPHNPs) F1, (b) LPHNPs F2, (c) LPHNPs F3, and (d) polycaprolactone polymeric NPs. (Scale bar:100 nm)

F3) was shown as  $68.433 \pm 1.7\%$ ,  $67.19 \pm 2.08\%$ , and  $72.693 \pm 1.8\%$ , respectively, and for PNPs, % drug release was  $92.81 \pm 0.04\%$  in 24 h. Therefore, it was observed that LPHNPs release the drug slowly than PNPs. The differences in % drug release between LPHNPs and PNPs were considered as statistically significant ( $P < 0.05$ , two-tailed unpaired student's *t*-test). The LPHNPs displayed a biphasic drug release pattern with an initial burst release, followed by sustained release. The reason for initial burst release profile may be due to the adherence of some of the nateglinide on the surface of LPHNPs. From the TEM images, it was observed that the polymer core of LPHNPs is surrounded by a lipid monolayer and the presence of this outer lipid layer acts as a rate-limiting membrane for the release of the encapsulated drug due to which sustained release is attributed.<sup>[49]</sup> The architectural structure of LPHNPs contributed to the controlled release of nateglinide. Therefore,

the *in vitro* drug release study demonstrated the more controlled delivery of nateglinide from LPHNPs.

To determine the mechanism of drug release from the LPHNPs and PNPs, the data obtained from *in vitro* release studies were fitted to various mathematical models such as zero order, first order, K-P model, and Higuchi model. The value of the correlation coefficient ( $R^2$ ) was calculated to determine the results of model fitting to the release data. The value of the correlation coefficient for drug release in phosphate buffer pH 6.8 is given in Table 4.

After evaluating the  $R^2$  value of all the kinetic models, it can be concluded that the drug release from LPHNPs (F1) and LPHNPs (F2) formulation mainly follow the K-P kinetic model which have a higher  $R^2$  value of 0.983 and 0.960, respectively. The value of diffusional release exponent in LPHNPs (F1) is 0.5, which indicate that the drug release is Fickian diffusion mechanism and in F2 the diffusional release exponent is 0.639 which indicate that it follow non-Fickian diffusion mechanism of drug release. The  $R^2$  value observed with LPHNPs (F3) indicates that the drug release is diffusion controlled and erosion of polymer matrix following Higuchi kinetic model. The drug release from PNPs also follows Higuchi kinetic model. The drug is released from the polymeric nanoparticle by the process of diffusion.<sup>[50]</sup>

The diffusional release exponent ( $n$ ) was calculated from the K-P drug release graph plotted as  $\log \% \text{ drug release}$  ( $\log M_t/M_\infty$ ) versus  $\log \text{ time}$  ( $\log t$ ). The slope of the graph is considered as  $n$ . When  $n$  approximates to 0.5, a Fickian/diffusion-controlled release is implied; where  $0.5 < n < 1.0$ , indicates a non-Fickian transport mechanism and for  $n = 1$ , indicates zero order (Case II transport) release mechanism. When  $n$  approaches 1.0, one may conclude that the release is approaching zero order.<sup>[51,52]</sup>

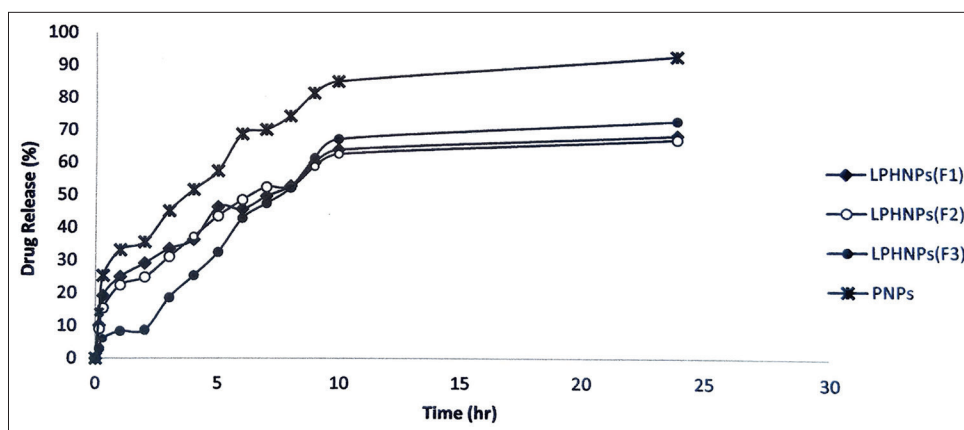


**Figure 7:** *In vitro* drug release profile of lipid-polymer hybrid nanoparticles (LPHNPs) F1, LPHNPs F2, LPHNPs F3 and polycaprolactone polymeric NPs

**Table 4:** Correlation coefficient ( $R^2$ ) of different kinetic models

Sl. No.	Formulation	Zero order model	First order model	Higuchi model	Korsmeyer–Peppas model	<i>n</i> -value
		$R^2$	$R^2$	$R^2$	$R^2$	
01	LPHNPs (F1)	0.687	0.792	0.927	0.983	0.509
02	LPHNPs (F2)	0.664	0.756	0.916	0.960	0.639
03	LPHNPs (F3)	0.743	0.819	0.893	0.772	1.017
04	PNPs	0.680	0.895	0.918	0.916	0.510

## CONCLUSION

The LPHNPs (NTG-PCL-GMS, NTG-PCL-PA, and NTG-PCL-LA) have been successfully developed by single ESE method and further characterized for various physicochemical parameters including particle size, entrapment efficiency, DL, compatibility of excipients, and crystalline behavior and *in vitro* drug release profile. The LPHNPs showed smaller particle size than PNPs ( $P < 0.05$ ). The hybrid NPs showed higher drug encapsulation and loading as compared to PNPs ( $P < 0.05$ ). From the TEM analysis, it was observed that LPHNPs attributed a polymer core with a surrounding lipid monolayer shell. The FT-IR, DSC, and XRD analysis showed the physicochemical compatibility of the particles and its components. The LPHNPs loaded with nateglinide showed slower drug release (60–70%) as compared to PNPs (90%) at 24 h ( $P < 0.05$ ). Among the three hybrid nanocarriers, LPHNPs F1 (NTG-PCL-GMS) is considered as the best combination for formulation due to their higher encapsulation ( $87.76 \pm 0.23\%$ ) and slower release of drug. In all LPHNPs formulations, drug was released by diffusion controlled mechanism. Based on the characterization and *in vitro* release profile, it can be concluded that the LPHNPs can provide controlled delivery of a hydrophobic drug nateglinide and act as a useful platform for drug delivery with improved pharmacokinetic profile. These LPHNPs are also suitable for the encapsulation of hydrophilic drugs. These hybrid NPs can also be utilized for the delivery of wide ranges of drug for the management of different diseases through different routes of administration. Hence, further studies are warranted

to compare its effectiveness with available marketed formulations.

## ACKNOWLEDGMENTS

The authors are thankful to Sophisticated Analytical Facilities, CSIR-NEIST, Jorhat, India, for providing facilities to conduct TEM analysis of the developed NPs.

## CONFLICT OF INTERESTS

The authors declare that they have no conflict of interests.

## REFERENCES

1. Hadinoto K, Sundaresan A, Cheow WS. Lipid-polymer hybrid nanoparticles as a new generation therapeutic delivery platform: A review. *Eur J Pharm Biopharm* 2013;85:427-43.
2. Zhang L, Chan JM, Gu FX, Rhee JW, Wang AZ, Moreno AF, *et al.* Self-assembled lipid-polymer hybrid nanoparticles: A robust drug delivery platform. *ACS Nano* 2008;2:1696-702.
3. Rizvi SA, Saleh AM. Applications of nanoparticle systems in drug delivery technology. *Saudi Pharm J* 2018;26:64-70.
4. Sailaja AK, Siddiqua A. An overall review on polymeric

- nanoparticles. *Int J Pharm Sci* 2017;2:21-8.
5. Ud Din F, Aman W, Ullah I, Qureshi OS, Mustapha O, Shafique S, *et al.* Effective use of nanocarriers as drug delivery systems for the treatment of selected tumors. *Int J Nanomedicine* 2017;12:7291-309.
  6. Ghasemiyeh P, Samani SM. Solid lipid nanoparticles and nanostructured lipid carriers as novel drug delivery systems: Applications, advantages and disadvantages. *Res Pharm Sci* 2018;13:288-303.
  7. Elsabahy M, Wooley KL. Design of polymeric nanoparticles for biomedical delivery applications. *Chem Soc Rev* 2012;41:2545-61.
  8. Kahraman E, Gung S, Ozsoy Y. Potential enhancement and targeting strategies of polymeric and lipid-based nanocarriers in dermal drug delivery. *Ther Deliv* 2017;8:967-85.
  9. Mandal B, Bhattacharjee H, Mittal N, Sah H, Balabathula P, Thoma LA, *et al.* Core-shell-type lipid-polymer hybrid nanoparticles as a drug delivery platform. *Nanomedicine* 2013;9:474-91.
  10. Mukherjee A, Waters AK, Kalyan P, Achrol AS, Kesari S, Yenugonda VM. Lipid-polymer hybrid nanoparticles as a next-generation drug delivery platform: State of the art, emerging technologies, and perspectives. *Int J Nanomed* 2019;14:1937-52.
  11. Krishnamurthy S, Vaiyapuri R, Zhang L, Chan JM. Lipid-coated polymeric nanoparticles for cancer drug delivery. *Biomater Sci* 2015;3:923-36.
  12. Wakaskar RR. General overview of lipid-polymer hybrid nanoparticles, dendrimers, micelles, liposomes, spongosomes and cubosomes. *J Drug Target* 2018;26:311-8.
  13. Chew WS, Hadinoto K. Factors affecting drug encapsulation and stability of lipid-polymer hybrid nanoparticles. *Colloids Surf B Biointerfaces* 2011;85:214-20.
  14. Garg NK, Tandel N, Jadon RS, Tyagi RK, Katore OP. Lipid-polymer hybrid nanocarrier-mediated cancer therapeutics: Current status and future directions. *Drug Discov Today* 2018;23:1610-21.
  15. Tentolouris N, Voulgari C, Katsilambros N. A review of nateglinide in the management of patients with Type 2 diabetes. *Vasc Health Risk Manag* 2007;3:797-807.
  16. Monteiro MS, Lunz J, Sebastiao PJ, Tavares MI. Evaluation of nevirapine release kinetics from polycaprolactone hybrids. *Mater Sci Appl* 2016;7:680-701.
  17. Raymond CR, Paul JS, Marian EQ. *Handbook of Pharmaceutical Excipients*. 6<sup>th</sup> ed. United States: Pharmaceutical Press and American Pharmacists Association; 2009. p. 383-474.
  18. Bachhav SS, Dighe VD, Kotak D, Devarajan PV. Rifampicin lipid-polymer hybrid nanoparticles (LIPOMER) for enhanced peyer's patch uptake. *Int J Pharm* 2017;532:612-22.
  19. Liu Y, Pan J, Feng SS. Nanoparticles of lipid monolayer shell and biodegradable polymer core for controlled release of paclitaxel: Effects of surfactant on particle size, characteristics and *in vitro* performance. *Int J Pharm* 2010;395:243-50.
  20. Dave V, Bala R, Kushwaha K, Yadav S, Sharma S, Agrawal U. Lipid polymer hybrid nanoparticles: Development and statistical optimization of norfloxacin for topical drug delivery system. *Bioact Mater* 2017;2:269-80.
  21. Gajra B, Dalwadi C, Patel R. Formulation and optimization of itraconazole polymeric lipid hybrid nanoparticles (lipomer) using box behnken design. *Daru* 2015;23:3.
  22. Tahir N, Madni A, Correia A, Rehman M, Balasubramanian V, Khan MM, *et al.* Lipid-polymer hybrid nanoparticles for controlled delivery of hydrophilic and lipophilic doxorubicin for breast cancer therapy. *Int J Nanomedicine* 2019;14:4961-74.
  23. Badri W, Miladi K, Robin S, Viennet C, Nazari QA, Agusti G. Polycaprolactone based nanoparticles loaded with indomethacin for anti-inflammatory therapy: From preparation to *ex vivo* study. *Pharm Res* 2017;34:1773-83.
  24. Kumar A, Sawant K. Encapsulation of exemestane in polycaprolactone nanoparticles: Optimization, characterization, and release kinetics. *Cancer Nanotechnol* 2013;4:57-71.
  25. Dave V, Kushwaha K, Yadav RB, Agrawal U. Hybrid nanoparticles for the topical delivery of norfloxacin for the effective treatment of bacterial infection produced after burn. *J Microencapsul* 2017;34:351-65.
  26. Ramesh G, Kumar SS. Formulation and characterization of noscapine-loaded polycaprolactone nanoparticles. *Asian J Pharm Sci* 2019;13:10-8.
  27. Devrim B, Kara A, Vural I, Bozkir A. Lysozyme-loaded lipid-polymer hybrid nanoparticles: Preparation, characterization and colloidal stability evaluation. *Drug Dev Ind Pharm* 2016;42:1865-76.
  28. Khan MM, Madni A, Torchilin V, Filipczak N, Pan J, Tahir N, *et al.* Lipid-chitosan hybrid nanoparticles for controlled delivery of cisplatin. *Drug Deliv* 2019;26:765-72.
  29. Thriveni T, Gangadharappa HV, Ravisankar P, Nair A, Leelavathi K. Formulation and evaluation of sustained release effervescent floating tablets of nateglinide. *IOSR J Pharm* 2018;8:45-54.
  30. Rima K, Dima M, Paolo Y. Polycaprolactone as drug carrier for an antifungal agent. *J Drug Deliv Ther* 2018;8:81-5.
  31. Jain AK, Thareja S. *In vitro* and *in vivo* characterization of pharmaceutical nanocarriers used for drug delivery. *Artif Cells Nanomed Biotechnol* 2019;47:524-39.
  32. Avinash A, Sushma A, Lalasa K, Kumar SP, Gowthami T, Sreenivasuls M. Design, characterization and evaluation of chrono-modulated nateglinide using pulsatile drug delivery system. *World J Pharm Biotechnol* 2016;3:1-6.
  33. Naik J, Lokhande A, Mishra S, Kulkarni R. Preparation and characterization of nateglinide loaded hydrophobic biocompatible polymer nanoparticles. *J Inst Eng India Ser D* 2017;98:269-77.

34. Wang J, Zhang L, Chi H, Wang S. An alternative choice of lidocaine-loaded liposomes: Lidocaine-loaded lipid-polymer hybrid nanoparticles for local anesthetic therapy. *Drug Deliv* 2016;23:1254-60.
35. Azandaryani AH, Kashanian S, Derakhshandeh K. Folate conjugated hybrid nanocarrier for targeted letrozole delivery in breast cancer treatment. *Pharm Res* 2017;34:2798-808.
36. Rena T, Wanga Q, Xua Y, Conge L, Goua J, Taosa X, *et al.* Enhanced oral absorption and anticancer efficacy of cabazitaxel by overcoming intestinal mucus and epithelium barriers using surface polyethylene oxide (PEO) decorated positively charged polymer-lipid hybrid nanoparticle. *J Control Release* 2018;269:423-38.
37. Ravi PR, Vats R, Dalal V, Gadekar N, Aditya N. Design, optimization and evaluation of poly- $\epsilon$ -caprolactone (PCL) based polymeric nanoparticles for oral delivery of lopinavir. *Drug Dev Ind Pharm* 2013;11:1-10.
38. Mukerjee A, Sinha VR, Pruthi V. Preparation and characterization of poly- $\epsilon$ -caprolactone particles for controlled insulin delivery. *J Biomed Pharm Eng* 2007;1:40-4.
39. Dash S, Murthy PN, Nath LK, Chowdhury P. Kinetic modeling on drug release from controlled drug delivery systems. *Acta Pol Pharm* 2010;67:217-23.
40. Hu H, Liu D, Zhao X, Qiao M, Chen D. Preparation, characterization, cellular uptake and evaluation *in vivo* of solid lipid nanoparticles loaded with cucurbitacin B. *Drug Dev Ind Pharm* 2013;39:770-9.
41. Kaleemuddin M, Srinivas P. Lyophilized oral sustained release polymeric nanoparticles of nateglinide. *AAPS PharmSciTech* 2013;14:78-85.
42. Guncum E, Islkkan N, Anlas C, Unal N, Bulut E, Bakirel T. Development and characterization of polymeric-based nanoparticles for sustained release of amoxicillin-an antimicrobial drug. *Artif Cells Nanomed Biotechnol* 2018;46:S964-73.
43. Yu F, Ao M, Zheng X, Li N, Xia J, Li Y, *et al.* PEG-lipid-PLGA hybrid nanoparticles loaded with berberine-phospholipid complex to facilitate the oral delivery efficiency. *Drug Deliv* 2017;24:825-33.
44. Lokhande A, Mishra S, Kulkarni R, Naik J. Development and evaluation of nateglinide loaded polycaprolactone nanoparticles. *Micro Nanosyst* 2015;7:43-8.
45. Shi K, Zhou J, Zhang Q, Gao H, Liu Y, Zong T, *et al.* Arginine-glycine-aspartic acid modified lipid-polymer hybrid nanoparticles for docetaxel delivery in glioblastoma multiforme. *J Biomed Nanotechnol* 2015;11:382-91.
46. Gopi G, Kannan K. Fabrication and *in vitro* evaluation of nateglinide-loaded ethyl cellulose nanoparticles. *Asian J Pharm Clin Res* 2015;8:93-6.
47. Li Y, Wu H, Yang X, Jia M, Li Y, Huang Y, *et al.* Mitomycin C-soybean phosphatidylcholine complex-loaded self-assembled PEG-Lipid-PLA hybrid nanoparticles for targeted drug delivery and dual-controlled drug release. *Mol Pharm* 2014;11:2915-27.
48. Yalcin TE, Tamer SI, Takka S. Development and characterization of gemcitabine hydrochloride loaded lipid polymer hybrid nanoparticles (LPHNs) using central composite design. *Int J Pharm* 2018;548:255-62.
49. Duan R, Li C, Wang F, Yangi JC. Polymer-lipid hybrid nanoparticles-based paclitaxel and etoposide combinations for the synergistic anticancer efficacy in osteosarcoma. *Colloids Surf B Biointerfaces* 2017;159:880-7.
50. Gouda R, Baishya H, Qing Z. Application of mathematical models in drug release kinetics of carbidopa and levodopa ER tablets. *J Dev Drugs* 2017;6:1-8.
51. Aguzzi C, Cerezo P, Salcedo I, Sanchez R, Viseras C. Mathematical models describing drug release from biopolymeric delivery systems. *Mater Technol* 2010;25:205-11.
52. Jalali MB, Adibkia K, Valizadeh H, Shadbad MR, Nokhodchi A, Omid Y, *et al.* Kinetic analysis of drug release from nanoparticles. *J Pharm Pharm Sci* 2008;11:167-77.

**Source of Support:** Nil. **Conflicts of Interest:** None declared.